AD-A054 964 AIR FORCE GEOPHYSICS LAB HANSCOM AFB MASS F/G 3/1
FINAL REPORT: SUPER HI STAR EXPERIMENT.(U)
FEB 78 R F PELZMANN
UNCLASSIFIED AFGL-TR-78-047 NL

1 OF 1
AD A054964

END
DATE FILMED
7-78
DDC

AFGL-TR-78-0047
ENVIRONMENTAL RESEARCH PAPERS, NO. 625

Final Report: SUPER HI-STAR Experiment

ROBERT F. PELZMANN, JR.

21 February 1978

OPTICAL PHYSICS DIVISION PROJECT 7670
AIR FORCE GEOPHYSICS LABORATORY
HANSCOM AFB, MASSACHUSETTS 01731

AIR FORCE SYSTEMS COMMAND, USAF

This report has been reviewed by the ESD Information Office (OI) and is releasable to the National Technical Information Service (NTIS).

This technical report has been reviewed and is approved for publication.

FOR THE COMMANDER

John Howard

Chief Scientist

Qualified requestors may obtain additional copies from the Defense Documentation Center. All others should apply to the National Technical Information Service.

Unclassified

SECURITY CLASSIFICATION OF THIS PAGE (When Data Entered)

REPORT DOCUMENTATION PAGE

READ INSTRUCTIONS BEFORE COMPLETING FORM

(14) 1. REPORT NUMBER: AFGL-TR-78-0047, AFGL-ERP-625

2. GOVT ACCESSION NO.

3. RECIPIENT'S CATALOG NUMBER (9)

(6) 4. TITLE (and Subtitle): Final Report: SUPER HI STAR Experiment.

5. TYPE OF REPORT & PERIOD COVERED: Scientific. Interim rept.,

6. PERFORMING ORG. REPORT NUMBER: ERP No. 625

(10) 7. AUTHOR(s): Robert F. Pelzmann, Jr

8. CONTRACT OR GRANT NUMBER(s)

9. PERFORMING ORGANIZATION NAME AND ADDRESS
Air Force Geophysics Laboratory (OP)
Hanscom AFB,
Bedford, MA 01731

10. PROGRAM ELEMENT, PROJECT, TASK AREA & WORK UNIT NUMBERS
62101F
(16) 7670 06 06 (17) 06

11. CONTROLLING OFFICE NAME AND ADDRESS
Air Force Geophysics Laboratory (OP)
Hanscom AFB,
Bedford, MA 91731

(11) 12. REPORT DATE: 21 Feb 1978

13. NUMBER OF PAGES: 19

14. MONITORING AGENCY NAME & ADDRESS (if different from Controlling Office)

15. SECURITY CLASS. (of this report): Unclassified (12) 20p.

15a. DECLASSIFICATION/DOWNGRADING SCHEDULE

16. DISTRIBUTION STATEMENT (of this Report)

Approved for public release, distribution unlimited.

17. DISTRIBUTION STATEMENT (of the abstract entered in Block 20, if different from Report)

DDC JUN 13 1978 RECEIVED F

18. SUPPLEMENTARY NOTES

Present address: NASA Ames Research Center
Moffett, CA 94035

19. KEY WORDS (Continue on reverse side if necessary and identify by block number)

Infrared
Astronomy
Celestial backgrounds

20. ABSTRACT (Continue on reverse side if necessary and identify by block number)

Numerical coadding of repeated scans of an attitude-stabilized rocket-launched cryogenic telescope has achieved the theoretical gain of N in signal-to-noise ratio. The 3 December 1975 flight of the telescope also demonstrated a sensitivity improvement nearly as large, resulting from the increased effective-integration time, while retaining the higher frequency response of the detectors to discriminate in favor of point sources. Several infrared sources in a 1.2 deg by 10 deg area around β Andromeda were measured at 11.0 and 19.6 μm, including two faint red galaxies (NGC 389 and NGC 393) and a number of unidentified objects.

DD FORM 1 JAN 73 1473 EDITION OF 1 NOV 65 IS OBSOLETE

Unclassified

SECURITY CLASSIFICATION OF THIS PAGE (When Data Entered)

beta micrometers

409 578

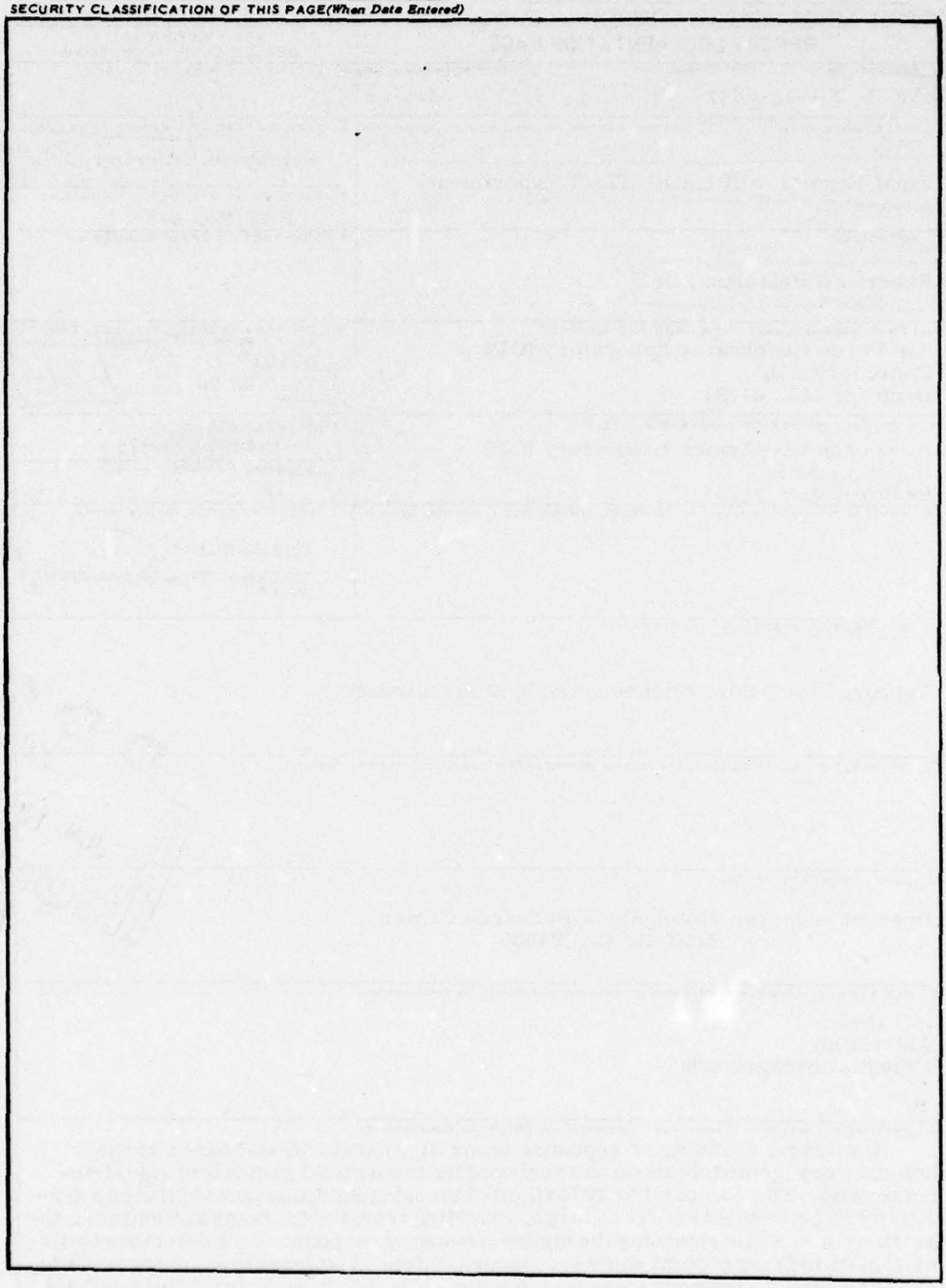

Contents

Illustrations

Tables

Final Report: SUPER HI-STAR Experiment

1. INTRODUCTION

The classical infrared technique of point-and-integrate used at ground-based telescopes for high-sensitivity photometry is not well suited to rocket-launched or satellite infrared systems, for several reasons. First, point-and-integrate requires a-c chopping of the optical path because of the unavailability of d-c amplifiers or photon-intregating detectors. Second, the resulting square-wave electrical signal requires large bandwidths in the radio telemetry system which constrain the number of detectors and the number of measurements that can be made. Finally, calibrating such systems in use and measuring more than one source places a heavy demand on the vehicle's attitude control system.

On the other hand, spatial coadding of multiple scans is a simple and straightforward extension of rocket sky-survey techniques in use since 1970. It allows a number of objects to be measured with little increase in system complexity, and theoretically achieves a sensitivity gain similar to the factor of the point-and-integrate technique. Furthermore, this sensitivity gain can be fully utilized in detecting weak sources without a priori knowledge of the source position, or even of its existence.

Spatial coadding offers three gains over familiar survey techniques, at the cost of a modified experiment program and a reduction of overall spatial coverage for the

(Received for publication 21 February 1978)

fixed experiment duration. First, for stationary uncorrelated gaussian noise, the signal-to-noise of significant sources is improved by $\sqrt{N}$. Here N is the total number of repeated scans of the source. Second, the total system sensitivity is improved by $\sqrt{N}$ divided by the degree of autocorrelation of the noise. Third, because multiple measurements of bright sources are made, the photometric uncertainty is reduced with a least-squares estimate of the amplitude; if the coadding is done properly, this best estimate is automatically produced.

However, achieving each of these three gains required separate considerations and techniques. Also, as with other rocket survey techniques, spatial coadding avails itself of the general benefits of digital measurement systems. That is, for the cost of computer software and processing time, very sophisticated statistical analysis techniques can be used to extract a maximum amount of information from the measurement. Furthermore, this can be done a postiori and be self-adapting to any operational problems, avoiding the need of constantly "tweaking" analog systems that in any case can never give more information than they were designed to give.

This report describes the advantages gained by coadding the scans of a cryogenic telescope that was rocket-launched on 3 December 1975 as a part of the Air Force Geophysics Laboratory's Infrared Sky Survey Program.

2. INSTRUMENT DESCRIPTION

2.1 Flight Payload

The Super-Hi-Star experiment payload was a modified version of the earlier Hi-Star system reported by Price and Walker.[1] For this mission, the zenith drive system was strengthened and a programmed control was added to allow scanning over a 10-deg range. A second axis star-tracker replaced the star-mapping sensor to provide spatially fixed attitude control so that a single area could be scanned repeatedly by the cyclic drive.

The payload consisted of a cryogenically cooled telescope mounted in a zenith gimbaled alt-azimuth system, the azimuth axis being aligned with the rocket roll axis. The nose cone, with blow-off covers, contained the two star trackers. The telescope mount was immediately below this; it had spring-loaded blow-off doors that would allow the telescope to be deployed to any zenith angle between 35 and 125 deg. The payload electronics occupied the section below the telescope yoke, followed by the attitude control system (ACS), the telemetry (TMS), and a piggyback experiment in the conical transition to the Aerobee-350 parachute recovery

1. Price, S. D., and Walker, R. (1976) The AFGL Four Color Infrared Sky Survey Catalog of Observations at 4.2, 11.0, 19.8, and 27.4 μm, AFGL-TR-76-0208, ERP No. 576.

system. This assembly was coupled to the rocket with a pyrotechnic separation ring that also carried the de-spin yo-yo weights.

The telescope was cryogenically cooled, configured as a doubly folded Gregorian, and had a 16.5-cm-diam primary aperture. It was equipped with internal baffles and stops, and had specially treated mirror surfaces to minimize radiation from the telescope structure onto the focal plane and to improve the instrument off-axis response. Interference filters were used over three portions of the focal plane, separated in the direction of scan, which permitted nearly simultaneous measurements in three broad spectral bands.

The focal plane contained a staggered linear array of eight detectors in each color band, with adjacent detectors in each array overlapped by one optical blur circle, as shown in Figure 1. The flat spectra effective wavelengths were 11.0, 19.6, and 27.4 μm, with bandwidths of 5.6, 6.0, and 3.4 μm, respectively. The individual detectors had instantaneous fields-of-view of 1.5 mrad in the scan direction by 3.05 mrad in the cross-scan direction. Cryogenic amplifiers and load resistors for each detector were located in the focal plane assembly to minimize electrical noise. The electrical signals were then further amplified and band limited by external amplifiers, sampled and digitized, and commutated onto the pulse code modulation telemetry system. The band-limiting amplifiers were optimized for point source response, giving a nearly symmetrical "S" signal shape for a stellar transit. The partially coadded results for β-Andromeda is shown in Figure 2.

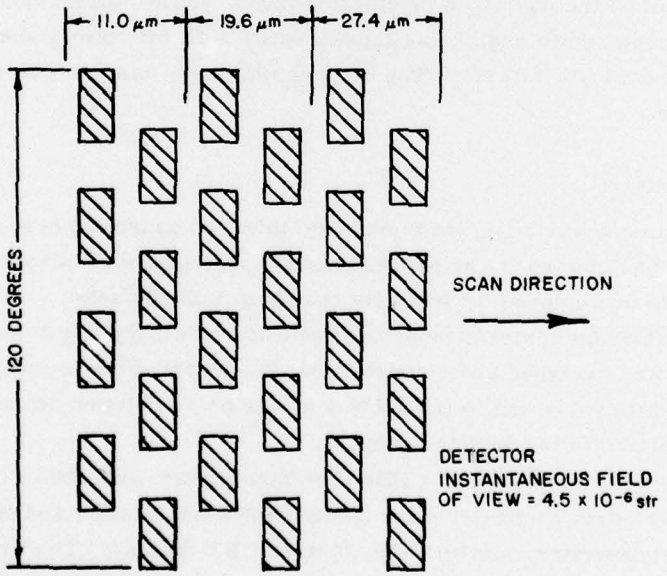

Figure 1. Super-Hi-Star's Detector Array Layout, Showing the Portions Covered by Each of the Three Interference Filters

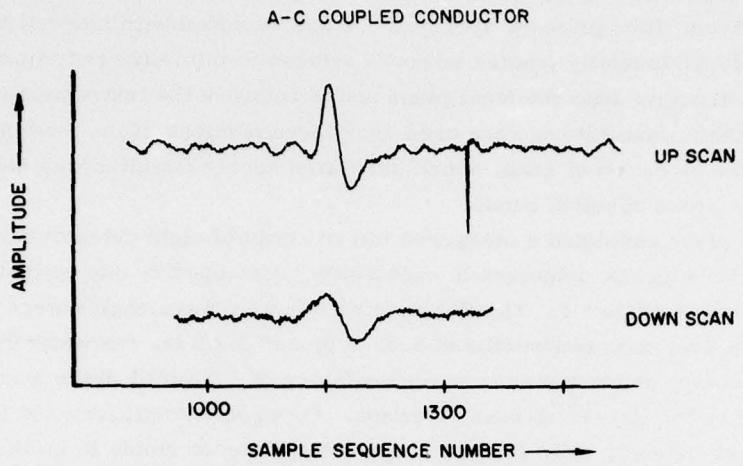

Figure 2. Coadded Point Source Signature for a Bright Source

The attitude reference and control of the vehicle was provided by the two star trackers. The digitized outputs of these sensors defined the direction of the two orthogonal-track axes to within 2 arc seconds. Additionally, the trackers provided the positional feedback information for the attitude control system that actively maintained the payload's orientation in the desired direction. The scan position (telescope zenith angle) was measured by a 13-bit optical shaft encoder mounted on the deployment axis. The deployment angle was measured to a fraction of 1 arc minute.

2.2 Ground Experiment

The experiment was designed to observe infrared sources whose signals would be too weak to be detected in the presence of the instantaneous sensor noise; the detection was to be achieved by spatially coadding multiple scans. In order to test the sensor performance prior to launch, a laboratory test facility based on a PDP-8 minicomputer was designed and constructed. Its purpose was to measure and control the system noise and to trace the sources of correlation and other non-gaussian properties in the detector outputs.

The test system consisted of a PDP-8 minicomputer with 4096 words of core memory, a seven-track tape drive for system software storage and control, an ASR-33 teletypewriter, and an 8- by 10-inch CRT display. The system also had a telemetry decommutator interface that was designed at AFGL especially for the Super-Hi-Star project. The software package developed included all coadder control routines and a set of statistical and calibration routines for data analysis.

2.3 Experiment Program

The mission observing time was divided into five segments:

- Immediately after the sensor deployed and began the oscillating scan, the roll position was to be offset by -0.65 deg and rolled +1.3 deg at 0.44 deg per sec. This would allow each of the eight detectors in each color to scan the central field star, β-Andromeda, several times, thus providing consistent calibration of all detectors during the flight.
- The roll position was to be recentered and scan data gathered until the sensor reached peak altitude.
- For 30 sec around the peak altitude, the scan oscillation was to stop and the focal plane shutter drive was to chop the optical path at a 1-Hz rate, to gather absolute background data.
- The scan oscillation was to resume and collect more coadding data on the scan region.
- The scan was to stop again and the chop sequence to run until the sensor was stowed for re-entry.

3. MISSION DESCRIPTION

The flight of A35.191-1 *was* successfully initiated at $03^h\ 21^m\ 59.^s 429$ GMT on 3 December 1975 (about 8:22 p.m. local time) from White Sands Missile Range. Performance and sequencing of the vehicle maneuvers occurred as planned. The roll axis pole star was ϵ Ursa Majoris, whose position is:

$$\alpha = 12^h\ 52^m\ 59^s$$

$$\delta = +56^\circ\ 05'\ 23''.$$

The side axis guide star and the central scan field star was β-Andromeda, whose position is:

$$\alpha = 1^h\ 08^m\ 23^s$$

$$\delta = 35^\circ\ 29'\ 37''.$$

The angular separation of these two axes is 88°.36. The position sensors tracking these stars exhibited a scan-driven cycling caused by the inertial reaction of the vehicle to the telescope's oscillating motion; this motion is shown in Figure 3 where

the motion of the vehicle has been resolved into the pitch and yaw axes, which were approximately + and -45 deg from the sensor scan axis. Thus the dual motion in pitch and yaw is actually a single motion reaction to the sensor scanning, whose period and phase agree exactly with the sensor motion. The amplitude of the cycling does not directly indicate the relative moments of inertia of the vehicle and the telescope because the ACS is actively damping the oscillations. (Thus the reaction is more nearly sinusoidal than the free saw-tooth motion.) This cyclic motion contributed to a correlated position error that affected the digital coadding and was compensated for as described in Section 4.

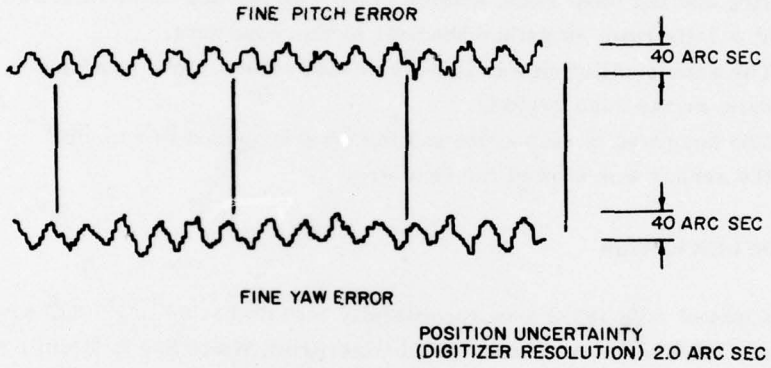

Figure 3. Performance of the ACS. The cyclic motion seen is response to the telescope's oscillating scan motion

The flight program sequence followed the expected plan with only two exceptions. Most significantly, a piece of debris from the payload remained near the rocket and occupied a portion of the scan field for most of the data-gathering period. This object was observed on the detector outputs immediately following sensor deployment as filling the entire field of view, and it appeared to recede erratically during the entire observing sequence.

Assuming that the object was larger than an individual detector, an emission temperature of 350°K was calculated from the in-band flux ratios. Unfortunately, during the chop sequence of the third and fifth experiment periods, the telescope was pointed directly at the object; therefore, no meaningful data were obtained on the absolute background brightness.

The erratic brightness measurements of the object during all the data segments could be the result of the object tumbling as it drifted away from the vehicle. It is not certain what the object was. Seven separate doors and covers were ejected

from the payload, but all of these releases occurred at low altitudes where aerodynamic effects should have swept all of them away. Additionally, the vehicle's flight orientation was such that the scan area was at the zenith, while all ejections occurred in horizontal directions before the payload was maneuvered to final orientation; it is difficult to understand how any of the doors could have been carried above the sensor.

A second possible source of the object is the sensor cover. The cover is removed from the telescope by a jack-screw mechanism before deployment, and it is replaced after the telescope is stowed for re-entry. This cover provides a vacuum seal of the optical system, and has an insulation pack of perforated mylar on its inner surface. If a portion of this cap or the insulation was loose, the deployment motion would have thrown it into the field of view at the lower edge of the scan. It would then recede slowly, remaining always at the lower edge of the scan field, exactly as was observed. Regrettably, the payload broke apart on re-entry when the recovery system malfunctioned. The sensor assembly was so severely damaged on impact that it was not possible to examine the cap for loose or missing material. Therefore, it is not possible to determine the origin of the stray object.

The second difficulty in the flight sequence was an erratic drifting of the roll position for the first 50 sec of the data-gathering sequence. The ACS system was initially not able to control this, although it did finally stop. This discrepancy has not been explained.

The sweep rate of the oscillating scan also increased about 3 percent during the experiment, probably due to warming of the drive motor and lubricants.

4. DATA REDUCTION

The Super-Hi-Star data reduction proceeded in two phases. First the data were pre-conditioned; that is, the cyclic scans were coadded in a manner that maximized the spatial correlation. This required the highest possible degree of positional accuracy. Correlated noise was removed to some extent, and the resulting spatial stream was digitally filtered to optimize the point source response.

Second, the point sources were extracted, using techniques similar to those used during previous AFGL Sky Survey programs.[1] It was necessary to compensate the source selection routines for unexpected data anomalies, including the very bright, extended signature of the near field object, and for a significant degree of spatially correlated noise. For the 11.1 and 19.4 μ channels, this correlated noise was probably caused by acoustic coupling from the gear system in the scan drive mechanism. The 27.4 μ channels exhibited an additional correlated signal of undetermined origin, which is discussed below.

Spatial coadding was the most complicated task of the data processing. For very bright signals, such as that seen for β-Andromeda in the center of the scan field, only a moderate degree of spatial accuracy was needed. This signal had a very large signal-to-noise ratio (S/N), and covered nearly 100 samples. Since individual samples are separated by only a few arc seconds, time sequence coadding was sufficient to achieve 75 percent of the theoretical $\sqrt{N}$ gain in S/N for this signal.

However, β-Andromeda was the only bright celestial source in the scan field. In order to detect sources with signals small compared to the instantaneous sensor noise, spatial correlation of a very high accuracy was needed. Since it was possible for a point source to have only four samples discernable from the final noise, scan to scan correlation better than 10 arc seconds was needed. Three elements of the vehicle attitude system were used to achieve this:

- The active altitude system held the vehicle stable to a fraction of an arc minute. This kept all positional variations smaller than a detector's instantaneous field-of-view, so that each detector's data stream could be treated independently of the others. It also permitted the use of first-order approximations for all positional corrections, which kept the consumption of computer time within reason.
- The digitized output of the optical shaft encoder was used to locate the direction of the telescope at the time of each sample. The resolution of the shaft encoder was such that approximately three samples occurred between successive values of the encoder readout. However, the scanning drive system had been constructed to better than 1 percent linearity, so that a first-order least-squares fit of the time and encoder readout gave a direction tag for each sample to better than 5 arc seconds (1 sigma variance).
- As shown in Figure 3, the vehicle reaction to the scan motion was larger than the resolution of the shaft encoder. Using the output of the attitude control system, the geometric transformation was made to compensate each sample's position for the cyclic and non-cyclic motion of the payload. First-order approximations of the coordinate transformation were found to be adequate to correct for the 40-arc-second cyclic excursions.

The data stream from each detector was thus spatially correlated to very high resolution; these samples were coadded in 8-arc-second bins, with an independent count of the number of samples in each bin and separate sequences for "up" and "down" scans. This count was needed for two reasons: First, although the scan drive remained very linear throughout the flight, the scan rate varied from scan to scan. This variation was predominantly a monotonic increase in the scan speed due to warming of the drive system, and it amounted to about a 3 percent change

from the beginning to the end of the data period. Because of this, a steady decrease in the number of samples per scan occurred. Second, such a count was needed to minimize the correlation figure of the system noise and to give a statistical best estimate of the correct normalized measurements. The sequence of spatial bins was normalized by the number of samples in each bin and the output was normalized to the source detection phase.

Figure 4 shows the effect of an increase in signal to noise for a dim source by increasing coadding and number of scans.

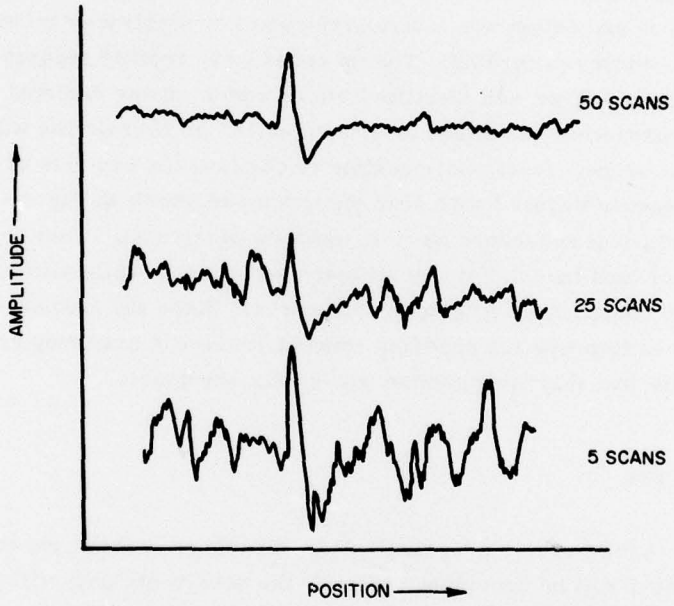

Figure 4. The Effects of Weak Source Extraction by *Coadding*. Here each plot is normalized by the number of scans coadded, so that the signal remains constant while the noise should decrease by $\sqrt{N}$

Because of the variation in scan rate, the frequency content of the data stream was not constant. Compensation by digital filtering of the raw data on the basis of the scan rate was tested and found to be unnecessary for adequate point source discrimination, as the band pass of the raw data had been set somewhat wider than necessary. Filtering of the coadded data was sufficient to optimize the point source response. Additionally, complete filtering of the raw data would have increased the data processing time by at least 20 percent. Since the coadding described required

12,324 seconds of central processor time (over 3-1/2 hours) on the AFGL Control Data Computer System, such an increase was not justifiable. (Only a small effort was made to minimize the run time of the computer programs, so that the indicated run time is only a rough estimate of what should be needed.) Radiation hits were found in the data stream, with large pulses occurring at the rate of one or two per second. As with previous missions, these could be discriminated by their very rapid rise rate. Additionally, since the same area was being scanned repeatedly, any bright signal seen only once was obviously not real; this fact was used to optimize the hit rejection routine. These pulses were detected in the raw data stream. Where one was found, the input data was omitted from the scan while the voltage excursion completed its rise to peak, undershoot, and the subsequent rise to within 3 sigma of the prior baseline.

Point source extraction was a straightforward application of techniques used on other AFGL survey programs. The up scans were treated separately from the down scans, and a source was identified where a source was detected in both directions; source extraction was based on S/N value and on correlation with the unexpected signal shape. It was not possible to combine the two sets of data because the system response differed with scan direction, as shown in Figure 2, and also because the temporal sequences were in opposite directions. This approach sacrificed a factor of less than 1.4 in the ultimate sensitivity, while allowing a similar increase in the confidence estimate of the source. Since the primary mission of the program was to prove the coadding concept, rather than survey at the highest possible sensitivity, this compromise was easily acceptable.

5. FINAL RESULTS

The final results of this program will be discussed in three phases: First, the S/N improvement will be described; second, the sensitivity gain will be discussed; and, finally, the region surveyed and sources detected will be covered.

As mentioned previously, in order to achieve the expected $\sqrt{N}$ improvement in S/N, the correlation accuracy must be comparable to the signal rise time. For bright signals, this requires spatial accuracy to about 1/2 arc minute. If the resulting coadded output is normalized by the number of scans, then the peak-to-peak height of a real signal will remain constant. If, on the other hand, the normalization factor is $\sqrt{N}$, then the rms noise should remain constant and the signal grow by $\sqrt{N}$. Figure 4 indicates that in the first case the signal does indeed remain approximately constant. (For bright signals, the consistency of normalized amplitude is better than 95 percent.)

Figure 5 shows the results of the second case for the rms noise of four of the detectors in each color; the other four detectors are omitted for clarity, and do not

disagree in any way with the data presented. The 11.0 μ channels are almost ideal in the noise reduction. The unusually large value of noise for small N on channel 1 is due to telemetry spike. It is a benefit of spatially correlated coadding that such anomalous errors are averaged away, as can be seen in the top graph of Figure 5.

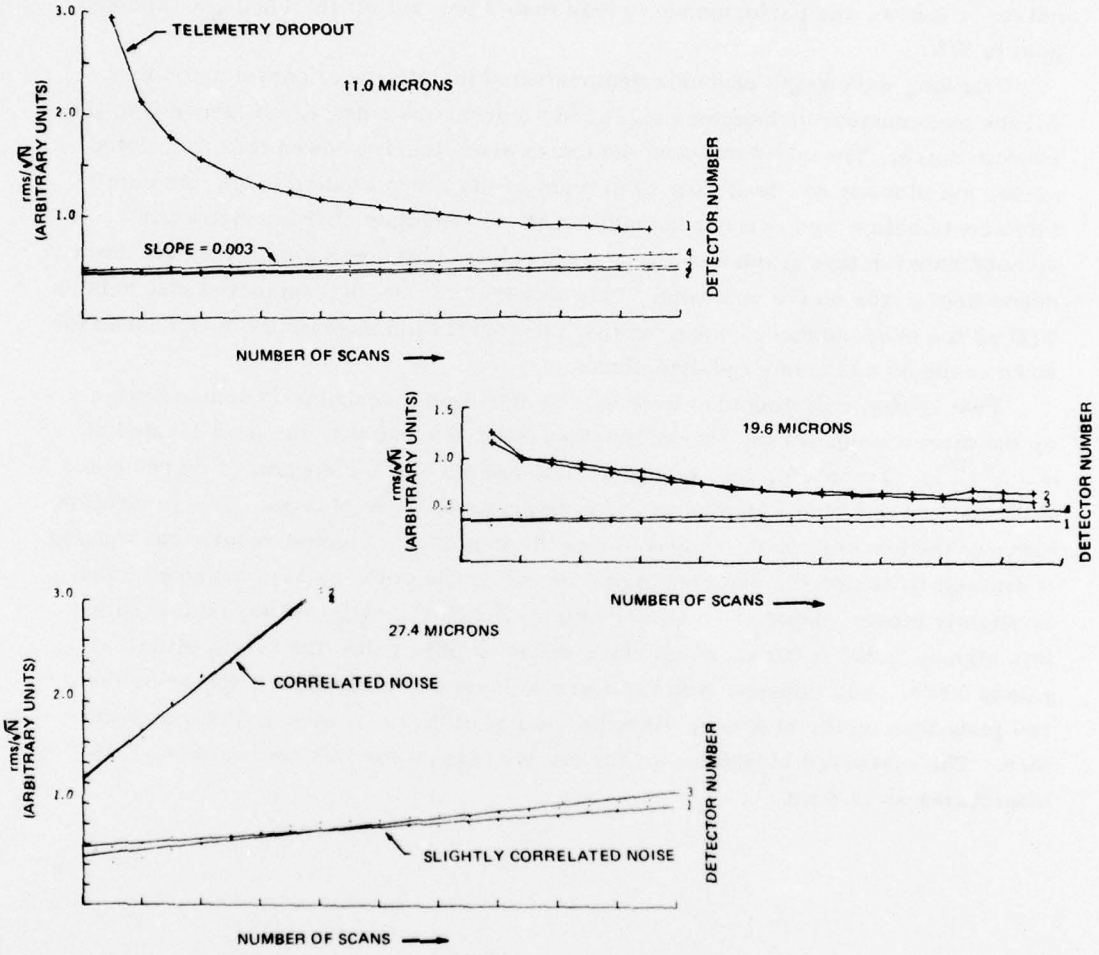

Figure 5. The Noise Performance for the Three Colors, as Described in the Text. Here, the noise is normalized by $\sqrt{N}$, so that ideal performance occurs if the noise figure is constant

The middle graph shows the noise performance of the 19.6 μ channels. Again, detectors 2 and 3 have an anomalous event, in this case a radiation spike that occurred on both channels in the first scan. The effect of this had already decayed significantly by the beginning of the graph, and was almost negligible by the end of the data sequence. The slight increase in the normalized noise level as the number of scans increased was due to the incomplete removal of the correlated gear drive noise. Even so, the performance is less than 2 percent off the ideal $\sqrt{N}$ expected gain in S/N.

The long wavelength channels demonstrated the effects of correlated noise. All the even numbered detectors exhibited a correlated noise much larger than the random noise. The odd-numbered detectors also clearly showed this correlated noise, but since it was less than 20 percent of the random noise level, the correlated contribution was correspondingly smaller. Another characteristic not demonstrated in this graph was that the correlated noise was smaller on the down scans than it was on the up scans. This was true for the odd numbered channels as well as the even numbered ones, so that the correlation essentially disappeared for down scans on odd numbered detectors.

That spatial coadding also lowered the detection thresholds is demonstrated by the measurement of the pair of galaxies NGC 389 and 393, the first located at $\alpha = 1^{n}7^{m}.1$, $\Delta = 39°34'$, the second 2' to the south (1975.0 epoch). Figures 6 and 7 show the red and blue Palomar sky survey prints of these objects. The separation between the two objects is comparable to the individual detector resolution, making it difficult to assign the detected signal to one or the other galaxy, although N393 is slightly closer; there are no other objects nearby likely to be associated with this signal. N393 is also a much more extended object than the bright elliptical galaxy N389. Additionally, N393 appears at least one magnitude brighter on the red plate than on the blue one, allowing the possibility of a strong infrared signature. The measured brightness of the coadded signal for this source was +1.45 magnitudes at 19.6 μm.

Figure 6. The Palomar Red Print of the Region Near N389, N393

Figure 7. The Blue Print of the Same Region. Note that N393 is much dimmer on blue, implying a large infrared excess

6. SOURCES OBSERVED

Table 1 lists the observed sources, their positions, and their brightnesses. Because of the correlated noise on the 27.4 μ channels, no measurements of sufficient confidence were made at this wavelength. Also, because of the near field object in the lower portion of the scan, the total area covered was reduced from the planned 1.2° × 10° to about 1.2° × 7.3°. Of the eight sources listed for this 8.7 square degree area, only one is bright enough to have been seen in the AFGL survey. That one is, of course, β-Andromeda, the field calibration star.

Table 1. Sources Observed

No.	RA(1950)	DEC(1950)	M(11)	M(20)	Remarks	Ch
1	1 3 50	40 9	-	0.89		4
2	1 4 30	37 15	2.17			2
3	1 5 35	39 27		1.45	N389/N393	6,7
4	1 5 45	37 21		0.65		4
5	1 6 30	38 00		1.21		6
6	1 6 35	38 55		1.00	E.O.	7,8
7	1 6 45	35 27	-2.05	-2.10	Beta And	4
8	1 8 0	36 9	2.70			7

Calibration of this source was made in December 1973 by the University of Wyoming, giving reference values of:

$-2^{m}.05$ at 11.0 μ m

$-2^{m}.10$ at 19.6 μ m

$-2^{m}.1$ at 27.4 μ m .

Because of the high background level during the calibration sequence, the channel-to-channel responsivities used to calibrate the measurements listed in the table were taken from pre-flight laboratory measurements.